Correcting the stress-strain curve in hot compression test using finite element analysis and Taguchi method

J. Rasti[1]*, A. Najafizadeh[2] and M. Meratian[3]
Department of Materials Engineering, Isfahan University of Technology, 84156-83111 Isfahan, Iran

Abstract
In the hot compression test friction has a detrimental influence on the flow stress through the process and therefore, correcting the deformation curve for real behavior is very important for both researchers and engineers. In this study, a series of compression tests were simulated using Abaqus software. In this study, it has been employed the Taguchi method to design experiments by the factors of material flow curve and the friction coefficient. The compression test was simulated up to the axial strain of 1 and then the deformation curve was extracted from the force-displacement plot of the strokes. Deviations between the deformation curves and the material flow curves were analyzed using Taguchi approach. Furthermore, the final shape of samples and friction coefficients were logically correlated. As a result, a new method was proposed in order to evaluate the material flow curve, based on the experimental data by the mathematical data manipulation..

Keywords: Hot compression test, Friction, Stress strain curve, Taguchi method.

1. Introduction
A compression test was carried out under frictionless conditions at which the test specimen deformed uniformly; so no barreling is occurred. In this condition, the obtained deformation curve based on force-displacement plot of the stroke is perfectly coincided to the material flow curve. In other words, any element in the sample behaves similar to the whole specimen deformation (Fig. 1).

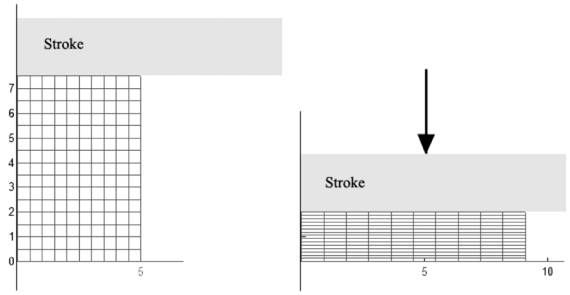

Fig. 1. The homogenous deformation during frictionless condition; any element in the material behaves the same as the bulk specimen during deformation

However, in conventional hot compression tests, friction leads to the heterogeneous deformation and develops three zones of deformation in the specimen as follows: (Figs. 2a and b) [1].
1) Dead-metal zone (DMZ) in which metal in contact with the top and the bottom of surfaces of the compression platens remains almost stationary.
2) Moderate deformation zone near to the outer surface of the specimen.
3) Intense shear zone in which the most severe deformation is concentrated in zones just outside the DMZs.

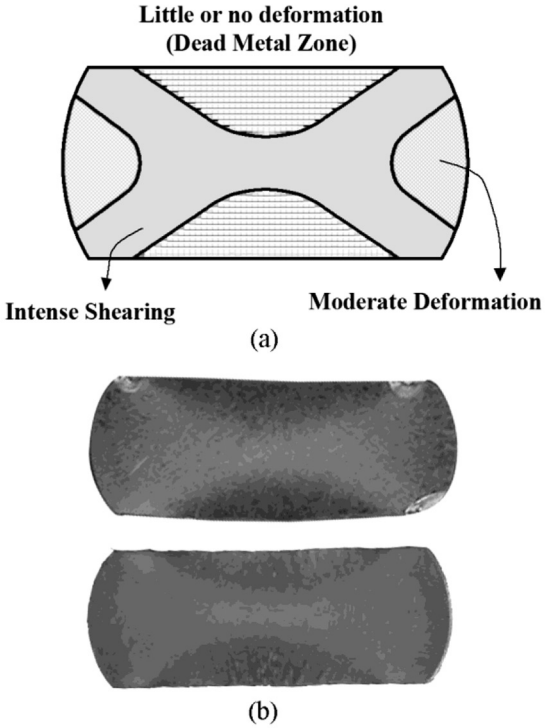

Fig. 2 (a) Different deformation zones developed in a specimen under hot compression test condition. [1] (b) Experimental evidence for the existing of these zones in a hot compressed material (macro-etched electrically in saturated nitric acid).

*Corresponding auther:
Tel: +98 (912) 1510654 Fax: +98 (311) 3912752
E-mail: j.rasti@ma.iut.ac.ir
Address: Department of Materials Engineering, Isfahan University of Technology, 84156-83111 Isfahan, Iran.
1. Ph.D. student
2. Professor
3. Associate Professor

The development of mentioned zones was carried out during three stages (Fig. 3) [1,2]. During early stage of the compression, lubricant near to the edge runs out, the edge of the workpiece then makes severe contact with the platens leading to initial barreling of the sample. While the compression continues and the specimen expands laterally, the material which was originally on the vertical sides of the specimen folds onto the compression platens, forming more unlubricated area. At the final stage, once the DMZs at the top and bottom of the sample come into contact, outward expansion of the end face begins, leading to severe radial plastic strain occurrence at the mid-height of the specimen. Logically, finer grain structure may be formed due to the severe plastic deformation in this region [3].

Besides, chilling effect and flow localization can also promote deformation heterogeneity. Chilling effect can arise when processing tool is colder than the workpiece; thus, heat is extracted throughout the tools. Consequently, the flow stress close to the interface is higher because of lower temperature. Flow localization results from the flow softening (against strain hardening) due to the deformation heating or generation of a softer texture or the dynamic recrystallization (DRX) occurred during deformation [1,4]. Under the condition of flow localization, deformation curve (the stress-strain curve obtained experimentally) is not necessarily coincided with material flow curve (the representative stress-strain curve in the frictionless condition) and some deviations are inevitable. Since the material flow curve reflects some intrinsic mechanical properties relevant to the certain microstructural features, its exploration is of great importance in these cases.

Basically, in the hot compression process, it is difficult to eliminate friction completely even using the lubricant between the sample and anvil surfaces [5]. Reducing friction coefficient brings deformation curve and material flow curve together, but some corrections are still needed.

Researchers often simply assume that friction coefficient is constant or independent of the strain level [6–10]. In their studies, the average friction coefficient has been evaluated through the measurement of barreling [10,11] or inverse analysis [12–14]. It is difficult to apply the inverse analysis methods universally in the hot working processes.

Recently, the method of Ebrahimi et al. [10] based on the measurement of barreling has been widely used to correct the stress-strain curve in a conventional compression test. In Fig. 4, deformation patterns of material predicted by this method through barreling factor of b=1 has been compared schematically with the predicted one by the finite element analysis. As can be seen, important differences exist between the deformation patterns. Side folding over (SFO) and intense changing of the axial strain along the centerline can be observed only in the latter. Since the latter case is consistent with the experimental evidence (Fig. 2b) the method of Ebrahimi does not look accurately precise in order to correcting stress-strain curve during the hot compression test.

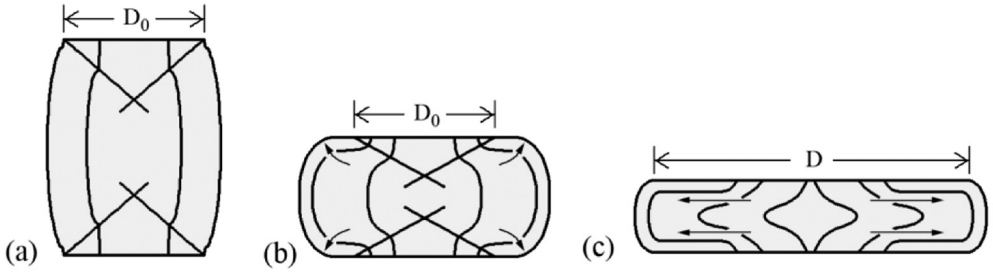

Fig. 3. Deformation pattern in the specimen under hot compression test. (a) The initial barreling. (b) Side folding over. (c) The expansion of the circumferential face. [1]

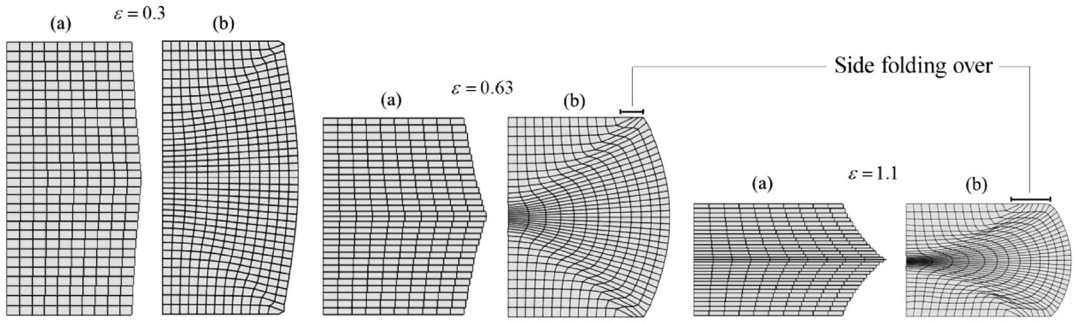

Fig. 4. Comparing the deformation patterns of material predicted by the; (a) Ebrahimi method through barreling factor of b=1 with, (b) that predicted by the finite element analysis at different stains.

In the present study, a series of compression tests were simulated using axisymmetric finite element method with Abaqus/Explicit package for a cylindrical sample. Input data included the material flow curve and friction coefficient, and the output data was the deformation curve obtained from the force-displacement plot of the strokes. The difference between material flow curves and deformation curves were analyzed using Taguchi approach. Also, the relation between the final shape of samples and friction coefficients was obtained. Consequently, by mathematical manipulation of data, a new method was proposed to extract the material flow curve from the experimental stress-strain curve during the hot compression test. To ensure validation, some experimental hot compression tests were performed under various frictional conditions and temperatures. The results showed this method would satisfactorily correct the stress-strain curves.

Taguchi technique is a design of experiments (DOE) method consisting of a plan for experiments with the objective of acquiring data in a controlled way. In this method, executing the experiments and analyzed data were executed, leading to obtain information about the behavior of a given process with the minimum number of tests. Basically, orthogonal arrays are used to define the experimental plans. More detailed information about this method can be found in references [15, 16].

2. Experimental Procedure

2.1. Design of experiments

Flow curves of materials with low to middle stacking fault energy such as austenitic stainless steels, copper, nickel, brasses [17], and ZK60 [18] alloys exhibit typical DRX flow curves with a single (or several) peak stress(es) followed by a gradual fall towards a steady state stress during the hot working [19]. Monotonic curves (curves with single peak stress) can usually be observed when the deformation temperature decreases and/or the strain rate increases. These curves can be characterized by some intrinsic points such as the peak stress (σ_p), the peak strain (ε_p), and the steady state stress (σ_s) (Fig. 5).

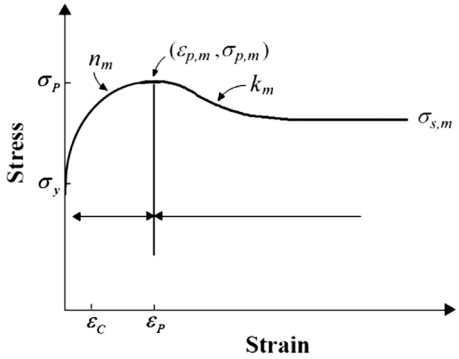

Fig. 5. The schematic diagram of a material flow curve for DRX: the curve can be characterized by four parameters n_m, $\varepsilon_{p,m}$, $\sigma_{p,m}$, and k_m. The parameters k_m and $\sigma_{s,m}$ were correlated through Eq. (3).

In some investigations, It has been developed constitutive equations for flow stress based on the metallurgical factors [20–22]. The stress–strain behavior up to the peak has been modeled using an equation as the following form [23–25]:

$$\frac{\sigma}{\sigma_p} = \left[\frac{\varepsilon}{\varepsilon_p}\exp\left(1-\frac{\varepsilon}{\varepsilon_p}\right)\right]^n \tag{1}$$

where σ is flow stress, ε the strain, and *n* is a constant obtained as follows:

$$n = \frac{\partial \ln(\sigma/\sigma_p)}{\partial\left(\ln(\varepsilon/\varepsilon_p)+1-\varepsilon/\varepsilon_p\right)} \tag{2}$$

Beyond the peak of the steady state stress, the following model has been presented [24]:

$$\sigma = \sigma_s + (\sigma_p - \sigma_s)\exp\left[k\left(\varepsilon - \frac{\varepsilon_p}{2} - \frac{\varepsilon^2}{2\varepsilon_p}\right)\right] \tag{3}$$

where the coefficient *k* can be calculated by selecting a point on the stress-strain curve before the peak (Eq. 1) in which $\varepsilon_k < \varepsilon_p$ and $\sigma_k > \sigma_s$, therefore:

$$k = \left(\varepsilon_k - \varepsilon_p/2 - \varepsilon_k^2/2\varepsilon_p\right)^{-1} ln\left(\frac{\sigma_k - \sigma_s}{\sigma_p - \sigma_s}\right) \tag{4}$$

In order to study the effects of material flow curve and friction coefficient on deformation curve (hereafter called the test stress−strain curve), Taguchi method was employed. A crucial step to use applying Taguchi approach is the selection of a proper orthogonal array. It was chosen a L_{16} (4^5) array containing 16 rows corresponded to the number of tests with 5 columns at 4 levels. The factors were assigned to the columns in Table 1.

Table 1. The orthogonal array L_{16} (4^5)

Test No.	Factor				
	σ_p	ε_p	*n*	*k*	μ
1	1	1	1	1	1
2	1	2	2	2	2
3	1	3	3	3	3
4	1	4	4	4	4
5	2	1	2	3	4
6	2	2	1	4	3
7	2	3	4	1	2
8	2	4	3	2	1
9	3	1	3	4	2
10	3	2	4	3	1
11	3	3	1	2	4
12	3	4	2	1	3
13	4	1	4	2	3
14	4	2	3	1	4
15	4	3	2	4	1
16	4	4	1	3	2

The input parameters for finite element analysis included: $\sigma_{p,m}$, $\varepsilon_{p,m}$, n_m and, k_m to define material flow curve and μ as friction coefficient. The levels that assigned 1 to 4 in Table 1 were related to the real parameter values in Table 2. It is noticed that σ_s can be calculated from the values of σ_p and k in each case (Eq. (4)). The output of the stress-strain curve obtained from finite element analysis was schematically shown in Fig. 6. The parameters define this curve which is consist of: the test of peak stress ($\sigma_{p,t}$), the test of peak strain ($\varepsilon_{p,t}$), the test of n value (n_t), the minimum test of stress beyond the peak stress ($\sigma_{min,t}$), the test of k value (k_t), and the stress at the strain of 1 ($\sigma_{\varepsilon=1}$). The schematic figure of final sample shape was also shown in Fig. 7 with two parameters namely radial strain of the sample at the contacted surface at the strain of 1 (ε_{CS}), and the ratio of the side folding over length to the contacted surface length (SFO/CS) at the strain of 1. The Taguchi approach was used to correlate these input and output parameters.

Table 2. Assignment of the levels to the factors.

Factor	Level			
	1	2	3	4
σ_p	80	110	140	170
ε_p	0.15	0.25	0.4	0.55
n	0.2	0.25	0.3	0.35
k	5	10	15	20
μ	0.1	0.2	0.3	0.4

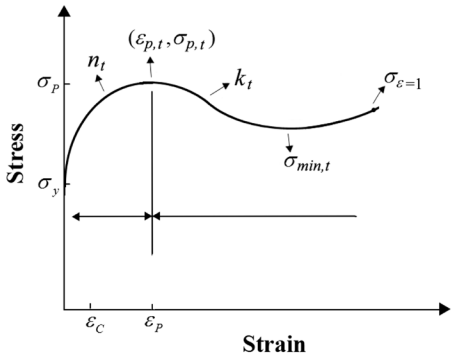

Fig. 6. The schematic diagram of a test stress strain curve obtained through hot compression process simulation.

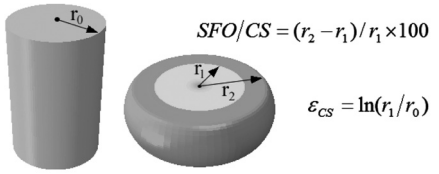

Fig. 7. The schematic figure of final sample shape after deformation with two parameters.

2.2. Materials

In order to validation of the proposed method some experiments were performed. It was used on AISI 304 stainless steel by the chemical composition of 0.033% C, 9.07% Ni. 18.3% Cr, 1.97% Mn, 0.342% Si, 0.573% Mo, 0.075% Ti, 0.023% P, and the balancing weight of Fe (wt%). Cylindrical samples with 15 mm in height and 10 mm in diameter were machined from the rolled bars. Hot compression tests were carried out in order to study recrystallization behavior during the deformation. Mica plates in both states with and without BN powder were used for two lubricated conditions. The initial grain size of samples was about 15 μm. Deformations were conducted at temperatures of 950-1100 °C under the constant strain rate of 0.005 s^{-1} up to strain of 1. Then friction coefficient and the material flow curve were determined based on the proposed model and consequently, they were inserted as the input data in the software. The compression test was simulated and simulated stress-strain curves were compared with experimentally obtained results.

3. Results and discussion

In Fig. 8, it has been shown four material-flow curves delineated at the mentioned conditions in Table 1. The corresponding simulated test stress-strain curves obtained from force-displacement plot of strokes and the samples' deformation patterns at the strain of 1 were also presented in Fig. 8. It should be noticed that if μ=0 (frictionless condition), then the curve of stress-strain test matched perfectly with the material flow curve, the deformation pattern was homogeneous, and no side folding over (SFO) existed.

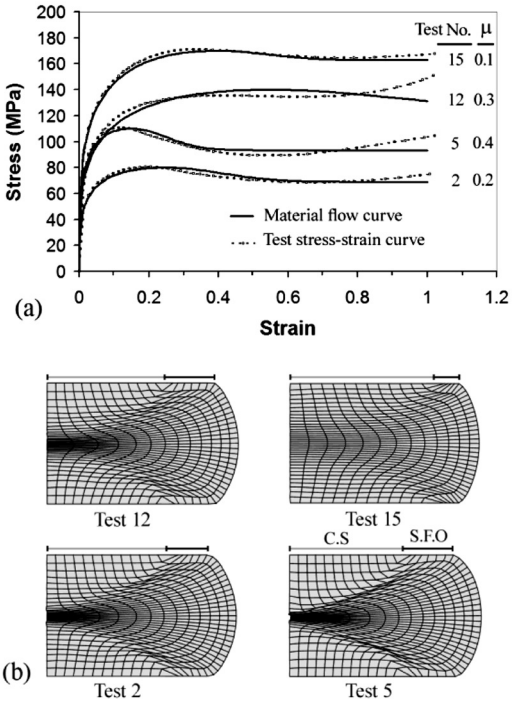

Fig. 8. (a) The material flow curves and simulated test stress-strain curves at the conditions mentioned in Table 1., (b) Corresponding samples' deformation patterns at the strain of 1; C.S=Contacted Surface, S.F.O=Side Folding Over.

There are some significant discrepancies between the curves of stress−strain test (SST curve) and the material flow curves (MF curve). They are:

1) Contrary to previous studies [10,11], no important change can be observed between the peak stress of two curves.

2) Peak strains of SST curve are somewhat lower than ones in MF curves. their difference is more pronounced with increasing peak strain and friction coefficient.

3) The stress rises as the compression continues to the high strains in SST curves. The amount of rising stress is related to friction coefficient and the peak strain values. The higher friction coefficient and the lower peak strain promote the relative volume of DMZ, concentrate the strain in the mid-height of the sample, and produce a high level hydrostatic compression stress resulting an increase in the applied stress at high strains.

Based on the average analysis, the Taguchi approach was employed to evaluate the effects of five already-mentioned factors, namely $\sigma_{p,m}$, $\varepsilon_{p,m}$, n_m, k_m, and μ (subscript *m* implies material flow curve), on the output of test parameters (Figs. 7 and 8).

In Fig. 9, it has been shown Taguchi average analysis for SFO/CS, ε_{CS}, $\varepsilon_{p,t}$, and ε_{max} in sample centerline. In this figure, both SFO/CS ratio and ε_{CS} value are dependent mainly on friction coefficient (μ). Increasing friction coefficient, the SFO/CS ratio increases and ε_{CS} value decreases. On the other hand, ε_{CS} value may be slightly increased by the peak strain of material. The peak strain of SST curve ($\varepsilon_{p,t}$) is mainly related to the peak strain of MF curve ($\varepsilon_{p,m}$) and friction coefficient. It must be noted that $\varepsilon_{p,t}$ is always smaller than $\varepsilon_{p,m}$. For example, when $\varepsilon_{p,m}$=0.55, the mean value of $\varepsilon_{p,t}$ becomes 0.5. This implies that SST curve shifts to the lower strain values rather than MF curve.

The above correlations helped to extract the following expressions for friction coefficient and the peak strain of MF-curve:

$$\mu = 0.04 ln\left(0.9\varepsilon_{p,t}^{0.25}/\varepsilon_{CS}\right) + 0.35\exp\left(0.046\frac{SFO}{CS} - 3\right) + 0.033\left(\sigma_{\varepsilon=1}/\sigma_{\min,t}\right)^{12.5} \quad (5)$$

$$\varepsilon_{p,m} = \varepsilon_{p,t}\exp(0.6\mu) \quad (6)$$

By a similar trend, the following relations was explored for the n_m, $\sigma_{p,m}$, and $\sigma_{s,m}$ (the steady state stress in MF-curve):

$$n_m = n_t \exp(-0.35\mu) \quad (7)$$

$$\sigma_{p,m} = \sigma_{p,t}\exp(0.04\mu(1+\varepsilon_{p,m})) \quad (8)$$

$$\sigma_{s,m} = \sigma_{\min,t}\exp\left(-0.01\sigma_{p,t}(\varepsilon_{p,m} - \varepsilon_{p,t}) + 0.22\mu\right) \quad (9)$$

$$\begin{cases} k_m = 7.14\left(\ln(k_t - 5) - 7\varepsilon_{p,t} - 5.4\mu + 2.3\right) & k_t > 5 \\ k_m \rightarrow \textit{from the Eq.}(4) & k_t \le 5 \end{cases} \quad (10)$$

k_t value can be calculated from the inclination of a straight trend-line crossed among the $\ln[(\sigma - \sigma_{\min,t})/(\sigma_{p,t} - \sigma_{\min,t})]$ *vs.* $(\varepsilon - \varepsilon_{p,t}/2 - \varepsilon^2/2\varepsilon_{p,t})$ data from $\sigma_{p,t}$ up to $\sigma_{min.t}$.

Once the hot compression test is performed on the cylindrical sample to the strain of 1, the curve of stress-strain test and the deformed sample shape can be employed to find friction coefficient (μ) (Eq. (5)) and the features of material flow curve such as $\varepsilon_{p,m}$, $\sigma_{p,m}$, n_m, $\sigma_{s,m}$, and k_m (Eqs. (6)-(10)). Then, the curve of material flow can be depicted using Eqs. (1) and (3).

Determining $\varepsilon_{p,m}$ and n_m, the critical strain related to the onset of dynamic recrystallization can also be calculated as follows [26]:

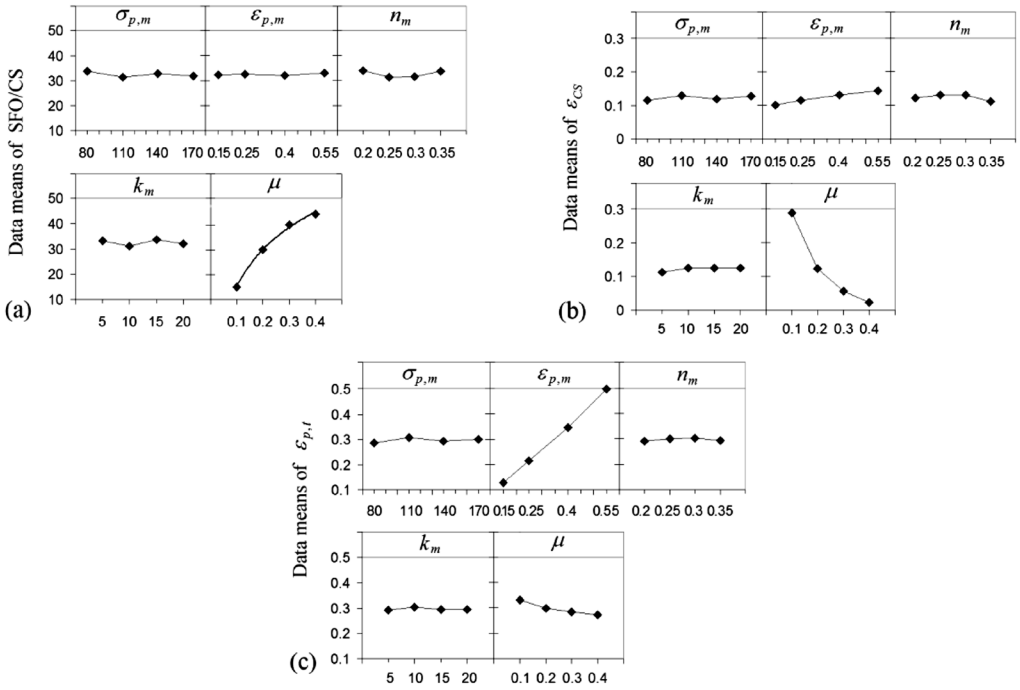

Fig. 9. Taguchi average analysis for; (a) SFO/CS , (b) ε_{CS}, and (c) $\varepsilon_{p,t}$ as functions of $\sigma_{p,m}$, $\varepsilon_{p,m}$, n_m, k_m, and μ.

$$\varepsilon_{c,m} = \left[1 - \frac{1-\sqrt{1-n_m}}{n_m}\right]\varepsilon_{p,m} \quad (11)$$

Two other important parameters were the maximum strain (ε_{max}) and the inclination, $(d\varepsilon/dx)_{\varepsilon max/2}$ of the axial strain along the centerline of the sample (Fig. 10(a)).

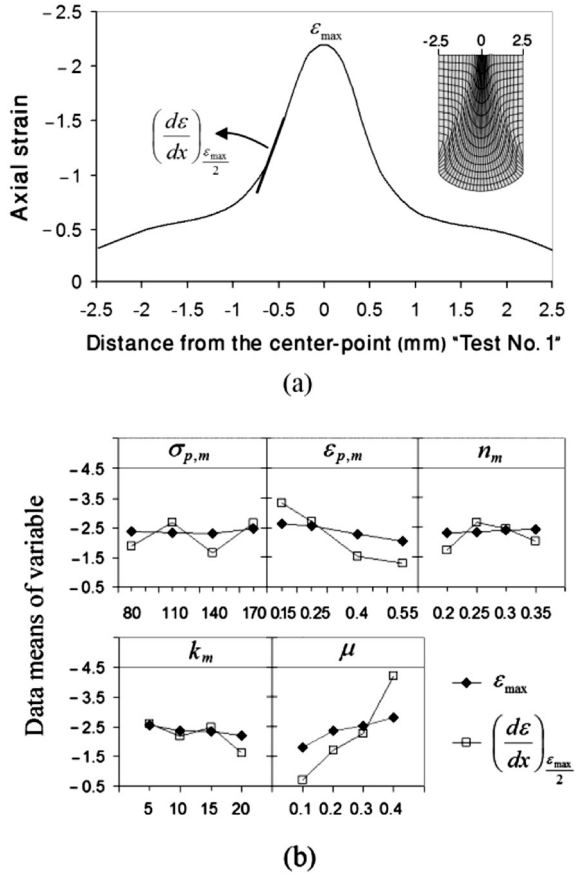

Fig. 10. (a) Variation of the axial strain along the centerline of the sample for the test number 1 (Table 1). (b) Taguchi analysis of the ε_{max} and $(d\varepsilon/dx)_{\varepsilon max/2}$ for all tests.

In Fig. 10(b), it has been shown the degree which parameters influence both ε_{max} and $(d\varepsilon/dx)_{\varepsilon_{max}/2}$. As can be seen, a decrease in peak strain and an increase in friction coefficient resulted in the promotion of ε_{max} and $(d\varepsilon/dx)_{\varepsilon_{max}/2}$ values. For example, ε_{max} approaches to -3 for cases of tests numbers 5, 13, and 14, while the bulk sample is imposed on the strain of -1.

4. Validation

In Fig 11(a)-(d) has been shown the stress-strain curves of samples deformed at the temperatures range of 950-1100 °C and the strain rate of 0.005 s^{-1} lubricated by just mica plate and mica plate + BN powder.

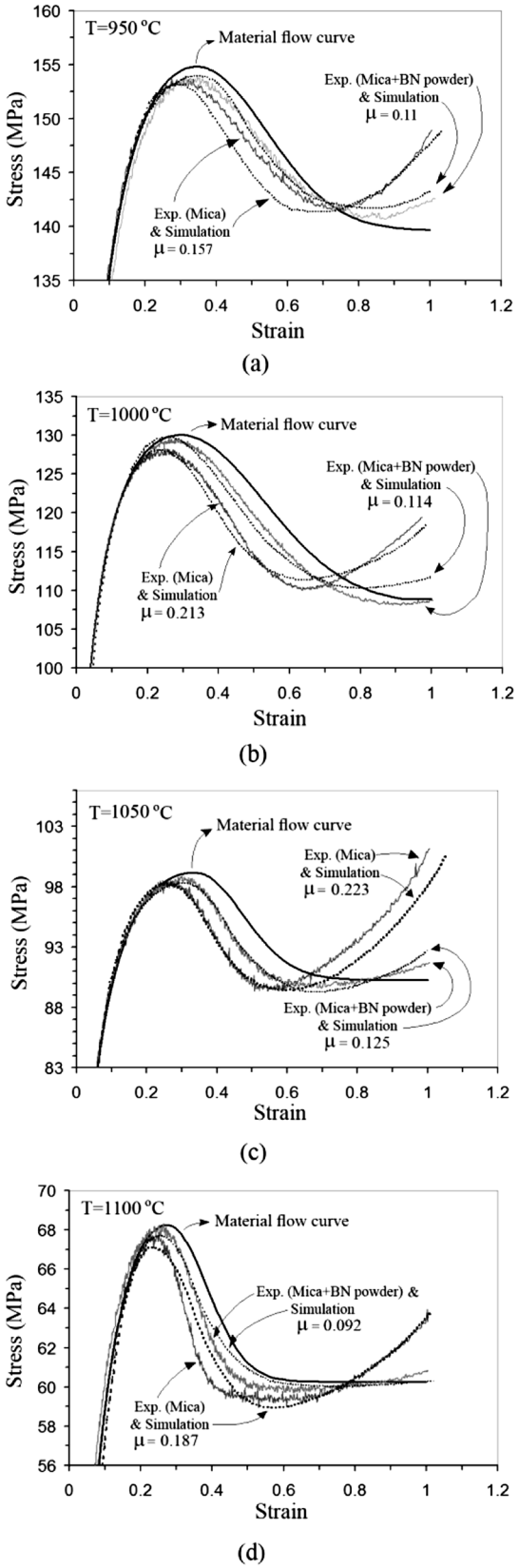

Fig 11. The stress-strain curves of deformed samples at the temperatures; (a) 950, (b) 1000, (c) 1050, and (d) 1100 °C under the strain rate of 0.005 s^{-1} with lubricants of the just mica plate and mica plate + BN powder.

Material flow curve and friction coefficient were extracted from the experimental stress-strain curve and final sample shape using Eqs. (1), (3), and (5)−(10). Then, data were inserted to the Abaqus software as the input data to simulate hot compression test. Simulated stress-strain curves were then compared with experimental ones in Fig. 9. The good coincidence between these two curves can be considered as a criterion to validate the proposed method.

Comparing the experimental stress-strain curve in the same deformation temperature and different lubricants indicates that as lubrication was performed more perfectly (the lower μ), peak strain and peak stress increased to the higher values. This implies that if test was conducted in a frictionless condition, where the test stress-strain curve coincided perfectly to the material flow curve, then higher measures of peak stress and peak strain were expected. Fig. 9 verifies it clearly.

In Fig. 12 the method of proposed correction in this study is compared with the suggested method by Ebrahimi et al. [10]. In Ebrahimi's method, because the power is required to compensate friction loss, the experimental stress-strain curve should be always settled higher than the curve of the frictionless condition. In other words, in order to obtain material flow curve, the correction of stress-strain curve is always accompanied with stress reduction.

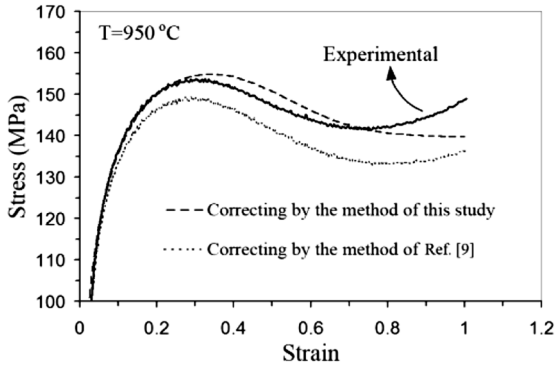

Fig. 12. Comparing the method of proposed correction in this study with the method of proposed by Ebrahimi et al [10].

On the other hand, once the non-homogenous deformation is also encountered, the work softening due to the dynamic recrystallization can be occurred somewhat sooner in some locations in which the strain accumulates (*i.e.* in the intense shearing zone). This may result in lowering the measure of applied stress. This indicates that in some situations, the compression strokes apply lower stress rather than the frictionless condition. Therefore, Material flow curve which is the representative curve for the frictionless condition may be settled somewhere above than the test stress strain curve.

5. Conclusion

The main conclusions drawn from the present study are:

- Relationships (Eqs. (5)−(10)) were proposed to determine the material flow curve (signed by *m* indice) using the experimental stress-strain curve (signed by *t* indice) and the deformed sample shape.
- Hot compression simulations showed that the peak strain and peak stress of the stress-strain curves obtained experimentally were somewhat lower than these peaks in the material flow curve. This discrepancy is related to strain concentration at the mid-height of the sample, due to friction, caused the DRX initiated at the lower strain in the sample and outmatched peak strain and stress.
- More friction coefficient and the lower peak strain caused strain accumulation in the mid-height of the sample was raised and the experimental stress increased more intense at the high level of strains.

References

[1] G.E. Dieter, H.A. Kuhn and S.L. Semiatin: Handbook of workability and process design, ASM International, USA, OH, (2003).

[2] W.F. Hosford and R.M. Caddel: Metal forming-mechanics and metallurgy, Prentice-Hall International, London, (1983),

[3] S.M. Fatemi-Varzaneh, A. Zarei-Hanzaki, M. Naderi and Ali A. Roostaei: J. Alloys and compod. 507 (2010), 207.

[4] F.K. Chen and C.J. Chen: J. Eng. Mater. Technol. (Trans. ASME), 122 (2000), 192.

[5] J.A. Schey: Tribology in Metalworking: Friction, Lubrication and Wear, ASM Int., Metals Park, OH, (1983),

[6] A.T. Male and V. Depierre: J. Lubr. Technol., 92 (1970), 389.

[7] F.P. Bowden and D. Rabor: The Friction Lubrication of Solid, First ed., Oxford University Press, London, (1950),

[8] H. Monajati, M. Jahazi, S. Yue and A.K. Taheri: Metall. Mater. Trans. A, 36 (2005), 895.

[9] R. Ebrahimi, A. Najafizadeh and R. Shateri: Proc. of Steel Symp. 81, Iranian Institute for Iron and Steel, Isfahan, Iran, (2003), 230.

[10] R. Ebrahimi and A. Najafizadeh: J. Mater. Process. Tech., 152 (2004), 136.

[11] Y.P. Li, E. Onodera, H. Matsumoto and A. Chiba: Metall. Mater. Trans., 40 (2009), 982.

[12] N. Kim and H. Cho: J. Mater. Process. Tech., 208 (2008), 211.

[13] H. Cho and T. Altan: J. Mater. Process. Tech., 170 (2005), 64.

[14] D. Szeliga, J. Gawad and M. Pietrzy: Comput. Methods Appl. Mech. Eng., 195 (2006), 6778.

[15] R.K. Roy: Design of experiments using the Taguchi approach-16 Step to product and process

improvement, Second ed., Wiley Interscience, New York, (2001),
[16] G.P. Syrcos: J. Mat. Process. Tech., 135 (2003), 68.
[17] E. El-Danaf, S.R. Kalidindi and R.D. Doherty: Metall. Mater. Trans. A, 30 (1999), 1223.
[18] A. Galiyev, R. Kaibyshev and G. Gottstein: Acta Mater., 49 (2001), 1199.
[19] H.J. McQueen and C.A.C. Imbert: J. Alloy. Compd. 378 (2004), 35.
[20] P. Dadras: J. Eng. Mater. Technol., 107 (1985), 97.
[21] C. Huang, E.B. Hawbolt, X. Chen, T.R. Meadowcroft and D.K. Matlock: Acta Mater., 49 (2001), 1445.
[22] Y. Lee, B.M. Kim, K.J. Park, S.W. Seo and O. Min: J. Mater. Process. Tech., 131 (2002), 181.
[23] A. Cingara and H.J. McQueen: J. Mater. Process. Tech., 36 (1992), 31.
[24] R. Ebrahimi, S.H. Zahiri and A. Najafizadeh: J. Mater. Process. Tech., 171 (2006), 301.
[25] E. Evangelista, M. Masini, M. El Mehtedi and S. Spigarelli: J. Alloy. Compd., 378 (2004), 151.
[26] R. Ebrahimi and S. Solhjoo: Int. J. of ISSI, 4 (2007), 24.